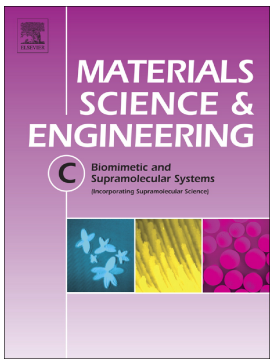

Quantum dots attached to graphene oxide for sensitive detection of ascorbic acid in aqueous solutions

Nandhini Arumugam, JongSung Kim

PII: S0928-4931(17)34527-7
DOI: doi:10.1016/j.msec.2018.07.017
Reference: MSC 8729

To appear in: *Materials Science & Engineering C*

Received date: 18 November 2017
Revised date: 23 June 2018
Accepted date: 7 July 2018

Please cite this article as: Nandhini Arumugam, JongSung Kim , Quantum dots attached to graphene oxide for sensitive detection of ascorbic acid in aqueous solutions. Msc (2018), doi:10.1016/j.msec.2018.07.017

Quantum dots attached to graphene oxide for sensitive detection of ascorbic acid in aqueous solutions

Nandhini Arumugam and JongSung Kim*

Department of Chemical & Biological Engineering, Gachon University

Seongnamdaero 1342, Sungnam-Si, Gyeonggi-Do 13120, Korea

*Correspondance: jongkim@gachon.ac.kr

Tel: +82-31-750-5361; fax: +82-31-750-5363.

Abstract

Water-soluble fluorescent carboxyl-functionalized CdSe-ZnS quantum dots (QDs) were immobilized on graphene oxide (GO) and used for sensitive detection of ascorbic acid in aqueous solutions. QDs were attached to the surface of graphene oxide using the EDC/NHS-sulfo coupling reaction. Ascorbic acid known as an antioxidant. It plays a crucial role in health maintenance, bio synthetic pathways such as formation of collagen and regulates immune system. The photoluminescence (PL) intensity of as-prepared GO-QD hybrids in water was quenched by ascorbic acid at ambient temperature. Based on this photoluminescence quenching phenomenon, a simple, rapid, and sensitive procedure is developed. In this study we are successful in detecting ascorbic acid due to its biological significance and the limit of detection is 568 pM.

Keywords: Ascorbic acid (AA); Graphene oxide (GO); Quantum dots (QDs); Biosensor

1. Introduction

Ascorbic acid (AA) or Vitamin-C is one of the important water-soluble vitamins, naturally present in citrus fruits and vegetables [1]. It performs an important biological role in humans and animals in processes such as the formation of collagen and the synthesis of neurotransmitters and carnitine [2]. In addition, it is a powerful anti-oxidant frequently used in the processing of food, pharmaceuticals, animal feed, and cosmetics. It is also used in clinical analysis: the level of AA in biological fluids can be used to analyze the extent of oxidative stress in human metabolism. It has been suggested that AA can counteract the common cold, cancer, mental illness, infertility, and some clinical manifestations of HIV infections [3]. Its deficiency leads to scurvy, while on the other hand "mega-dosage" consumption of Vitamin-C may result in problems such as urinary stones and diarrhea. [4]. Because of its importance, numerous analytical methods have been developed to detect AA, including electrophoresis [5], chemiluminescence [6], photoluminescence (PL) [7], and electrochemical techniques [8-12]. Among these, the PL method has been extensively studied because of its potential advantages of high sensitivity, simplicity, and low cost. Especially, many kinds of sensitive and selective researches have been performed to detect various organic molecules. [13, 14].

Semiconductor quantum dots (QDs) are inorganic nanoscale particles with special characteristics resulting from their size and the phenomenon of quantum confinement. Colloidal semiconductor QDs show interesting properties, such as a size- and composition-dependent emission wavelength, narrow emission band, broad excitation range, and very high stability against photobleaching [15]. For these reasons, QDs have numerous applications in areas such as biochemical sensing, labeling, cellular imaging, solar cells, LEDs, and diode lasers [16, 17].

Currently, graphene and other closely related carbon compounds, are attracting attention because of their superior electrical, thermal, and mechanical properties [16]. Among them, graphene oxide [GO] is a derivative of graphite, and has many specific characteristics that are widely different from graphite as a result of the oxygen-containing functional groups on the surface that produce a transparent, hydrophilic nature and also has a high specific surface area, tunable band gap, and good biocompatibility [19, 20]. In addition, GO has been considered as an excellent carbon material due to its superior mechanical strength [21], low density and high heat conductance [22]. Numerous applications have been developed based on graphene-polymer composites [23], batteries [24], fuel cells [25], drug delivery and biosensors [26, 27]. Especially, various GO functionalized nanomaterials/composites have been reported as novel nanosensors for sensitive, selective and rapid detection of different biomolecules, metal ions and drugs [28-34].

In the present study, we have prepared GO-QD hybrids as a biosensor for the detection of AA. The GO was used as a supporting substrate, with carboxyl-functionalized QDs attached to its surface. In this study, we synthesized GO by the modified Hummers' method, and linked QDs to the surface by the 1-ethyl-3-(3-dimethylaminopropyl) carbodiimide/N-hydrosuccinimide (EDC/NHS) coupling reaction to produce ester bonds. The carboxyl group of functionalized Cd/Se-ZnS quantum dots can be reacted with a GO hydroxyl group [35, 36]. Use of GO-QD hybrids as biosensors may be based on quenching of the PL intensity by various concentrations of AA.

2. Experimental

2.1. Chemicals and Materials

Qdot® ITK™ CdSe/ZnS carboxyl QDs were purchased from Life technologies, USA. Graphite flakes, H_2O_2, $KMnO_4$, H_2SO_4, ascorbic acid, 1-ethyl-3-(3-dimethylaminopropyl) carbodiimide (EDC), and N-hydroxysuccinimide (NHS) were purchased from Sigma-Aldrich, USA. HCl was purchased from Carlo Erba Reagents. Phosphate-buffered saline (PBS) was purchased from WelGENE Inc. All chemicals were directly used without further purification.

2.2. Instrumentation

The FTIR spectra were obtained using a Bruker VERTEX 70 high-resolution FTIR spectrometer, and the absorption spectra of the QDs were obtained with a Cary 100 UV/Vis spectrophotometer (Varian). High-resolution TEM (HRTEM) images were obtained with a transmission electron microscope (Tecnai G2 F30 S-Twin). Raman spectra were acquired using a Horiba Raman spectrometer (model T64000). X-ray diffraction (XRD) patterns of the particles were obtained using a Rigaku RINT 2200 diffractometer. Centrifugation was performed using a Thermo Scientific multifunction centrifuge. The PL spectra were recorded with an excitation wavelength of 450 nm at room temperature, using a photoluminescence spectrometer (QuantaMaster, Photon Technology International, NJ, USA) equipped with a xenon lamp (Arc Lamp Housing A-1010B, PTI), monochromator, and power supply (Brytexbox).

2.3. Preparations of GO and GO-QD hybrids

The GO was prepared from graphite flakes by the modified Hummers' method [37]. Briefly, 500 mg of graphite was mixed with 20 mL of concentrated H_2SO_4 in a 100 mL round-bottom flask with magnetic stirring for 4 h at room temperature. The reaction mixture

was cooled to -10 °C, and approximately 2.5 g of $KMnO_4$ was then slowly added; the reaction temperature was raised to 130 °C, and after addition of H_2SO_4 the solution maintained with vigorous magnetic stirring for 3 h. After the reaction, dark yellow GO was observed; the solution was cooled to room temperature and roughly 100 mL of DI water and 15 mL of 30% H_2O_2 were added. Finally, the GO was washed three times with 0.25 M HCl solution and centrifuged at 7,000 rpm for 15 min. GO-QD carboxyl-functionalized hybrids were prepared using the EDC/Sulfo-NHS coupling reaction. In one test tube, 20 mL of GO solution (250 mg/L) was mixed with 100 µL of 5 mM EDC and 100 µL of 7.5 mM NHS (both EDC and NHS solutions are in PBS buffer, 10 mM PO_4^{3-} at pH 7.2). In another test tube, 2 µL of 0.4 µM CdSe/ZnS-carboxyl QD solution was added to 250 µL of 5 mM EDC and 500 µL of 5 mM NHS in PBS buffer. Subsequently, 250 µL of QD solution was added to the above GO mixture and mixed with a vortex machine. The reaction mixture was kept at 8 °C overnight after 60 min of sonication. Finally, the GO-QD hybrids were isolated by ultracentrifugation at 10,000 rpm for 25 min, and washed with DI water three times. The GO-QD hybrids were dried under vacuum and stored at -4 °C for further analysis.

2.4. Fluorescence assay for ascorbic acid

AA was detected using a fluorescence assay as follows. In a typical procedure, 100 µL of various concentration of AA solution and 500 µL of PBS buffer solution were mixed and added to a cuvette containing 100 µL GO-QD carboxyl-functionalized hybrids. Different concentrations of AA were used, ranging from 0 to 130 nM. The mixture was incubated for 10 min at room temperature and PL spectra were recorded using an excitation wavelength of 450 nm.

3. Result and Discussion

The GO and GO-QDs hybrids were synthesized by using a modified Hummers' method and a coupling reaction, which we have illustrated in Fig. 1. After treatment of graphite with H_2SO_4 (conc.), $KMnO_4$, and H_2O_2, GO is present and has carboxyl and hydroxyl polar functional groups, which are confirmed by FTIR and Raman spectroscopy. The GO-QD hybrids were prepared by the EDC/Sulfo-NHS coupling reaction, which occurs through ester bond formation between carboxyl groups of the QDs and hydroxyl functional groups of GO.

3. 1. Characterization of GO-QD hybrids

Fig. 2 shows the FTIR spectra of graphite flakes, GO, and GO-QD hybrids. In the graphite sample, the characteristic sharp peaks observed at 680 and 1530 cm^{-1} are attributed, respectively, to the aromatic C-H and C=C stretching frequencies in graphitic carbon. In the GO and GO-QD hybrids, a broad and intense hydroxyl (O-H) peak at 3460 cm^{-1} and a strong C=O peak at around 1710 cm^{-1} result from stretching vibrations of carboxylic acid and carbonyl moieties, respectively. These clearly indicate that through COO bonding, the CdSe/ZnS QDs are well attached to the GO surface. Additional peaks are observed from GO at 1050 and 1235 cm^{-1} for C-O and C-O-C, respectively. The FTIR observation confirms the production of GO with polar functionalities and GO-QDs hybrid formation [38, 39].

The Raman spectra of GO, GO-QDs hybrid, and graphite are shown in Fig. 3. The G band is shown at 1597, 1607, and 1595 cm^{-1}, while the D band at 1365, 1364, and 1355 cm^{-1} for graphite, GO, and GO-QDs hybrids, respectively. The G band is common for all sp^2 carbon forms, and it indicates the C-C bond stretching. The G and D bands of GO are shifted to a higher wave number due to the oxygenation of graphite and structural defects, which results in the formation of sp^3 carbon atoms [40]. The Raman spectra of hybrids confirmed that the

grafting of QDs into the GO sheets resulting in a gradual reduction in the graphitic structure and thus decreased size of the graphitic domains. Therefore, the Raman spectral analyses show that the QDs has been well attached onto GO sheets [41].

To investigate the morphology of the GO-QDs, transmission electron microscopy (TEM) analysis was used. TEM images at different magnifications for CdSe/ZnS QDs, GO, and QD conjugated GO are shown in Fig. 4. In Fig. 4. (A), the QDs appear as dark dots of spherical shape, uniformly distributed on the surface. In Fig. 4. (B), GO alone appears as highly transparent and flexible wrinkled few layer of sheets. Fig. 4(C) and (D), shows well-conjugated QDs on the GO sheets at 100 and 200 nm magnifications, respectively [42, 43]. In addition, Energy –dispersive analysis of X-rays (EDX) was further used to reveal the elemental composition of C, O, Zn, S, Se, Cd and Cu (Cu comes from the TEM grid) for the as-synthesized GO-QD hybrids in Fig. 4(E). The HRTEM image of GO-QD hybrids (Fig. 4. (F)) shows the well resolved lattice fringes with a interlayer spacing distance of 0.36 nm, which clearly matches to the (1 1 1) crystal plane for QDs [44]. The selected area electron diffraction (SAED) pattern (inset in Fig. 4. (F)) displays a separated ring like feature, indicating polycrystalline nature of QDs.

Fig. 5 shows the UV-visible absorption spectra of GO and as-synthesized GO-QD hybrids. The trace for GO shows a strong absorption peak at about 230 nm indicating the $\pi \rightarrow \pi^*$ conjugated transitions of the aromatic C=C bond, and a small shoulder peak at about 300 nm indicating $n \rightarrow \pi^*$ transitions of C=O bonds [45]. For the GO-QD hybrids, the peak at 230 nm is red shifted to 270 nm by attachment of the QDs to GO.

The crystal structure of graphite, GO, and GO-QDs was investigated by powder XRD analysis. As shown in Fig. 6. The strong, sharp characteristic peak at $2\theta = 26.6°$ indicates a highly ordered structure in graphite. The trace for GO shows a strong peak centered at $2\theta =$

10.2° and a weaker peak around 2θ = 21°. The stronger peak results from oxygen-containing functional groups and the weaker one is the characteristic peak of residual unoxidized graphite [46]. However, the strong characteristic peak from GO is absent in the GO-QD hybrids, while the broad peaks at 2θ = 25.2 and 41° can be assigned to (111), (220) lattice planes of the CdSe/ZnS QDs [38].

3. 2. Effect of pH on PL emission of the QDs and time stability

It is known that the PL emission of CdSe/ZnS QDs is highly pH-sensitive; moreover, studies report the maximum PL intensity at different pH values [47, 48]. For CdSe-ZnS QDs attached to GO (this study), Fig. 7 shows the effect of pH on PL intensity for a pH range of 2–12. This Figure shows that the PL intensity at pH = 2 is about 20% of that at pH = 7.2. The acidic conditions may induce formation of surface defects, leading to aggregation of the GO-QDs and PL quenching. As conditions become more strongly basic (pH = 7→12), the PL intensity of the GO-QDs is quenched moderately (~20%), which may result from deprotonation by hydroxide ions (OH^-) at the surface [49]. Accordingly, in this study, the experiments on ascorbic acid sensing were carried out at a pH of 7.2. For long-term ascorbic acid sensing in biological environments, stability of the PL intensity is essential. Fig. 8 shows the stability of PL intensity of GO-QDs at room temperature. This Figure shows that the PL intensity remains constant for a duration of 100 h.

3. 3. Calibration plot and detection limit of the method

Fig. 9 shows the quenching of PL intensity from GO-QDs as a function of AA concentration. Various concentrations of AA from 0 to 130 nM were added to the GO-QD assay solution, and PL spectra were measured after a time interval of 10 min. The Figure shows that the PL intensity of GO-QDs gradually decreased with increasing AA

concentrations, which may result from electron transfer from the GO-QDs to AA. With an AA concentration of 130 nM, the PL emission has decreased to 20%. The inset Figure shows PL quenching as a function of AA concentration ranging from 0 to 130 nM. In addition, right side bottom of the inset figure also shows the photographic evidence for the PL quenching of GO-QDs by the addition of different concentrations of AA. In the Figure, F_0 and F are the PL intensity of GO-QDs in the absence and presence of a quenching agent (AA), respectively. Certainly, the PL quenching is closely related to the concentration of AA added to the GO-QDs solution. The well-known Stern–Volmer equation was applied to measure the relationship between quenching efficiency of QDs and concentration of AA [50].

$$F_0/F = 1 + Kq[AA] \qquad (1)$$

Here, K_q is the Stern-Volmer constant, representing the affinity between fluorophore and quencher. The figure shows a good linear relationship with correlation coefficient R^2 = 0.9941. The limit of detection (LOD) for AA was calculated to be as low as 568 pM. Finally, PL response was recorded in the presence of various potential interferences like biomolecules and ions, which were naturally present in our biological systems (Fig. 10). According to the PL data, except AA, significant fluorescence quenching was not observed from the biomolecules like uric acid, glucose, and citric acid after addition into the system as presented in Fig. 10A. In addition, we also recorded the PL response using our system with various existing ions (Fig. 10B). Interestingly, by addition of these ions into our sensing system, the fluorescence intensity was also remains almost same as like as GO-QDs, which clearly indicates that, the developed sensing probe is highly selective and sensitive towards the AA over the presence of various biomolecules and ions as potential interferences.

Several analytical methods such as electrochemical sensing, calorimetric sensing, and enzymatic immunoassays were available for the detection of AA [51-53]. However, in spite of having potential abilities by using these sensing systems, several disadvantages like sophisticated instrumentation handling, using of expensive chemicals, difficult reaction conditions, low limit of detection with selectivity were also associated from them. Herein, we developed an easy, economical, and simple fluorometric assay for the selective and sensitive detection of AA with low limit of detection. Moreover, this sensing system did not require much sophisticated instrumentation with specialized reaction conditions. As from the earlier experimental results, we performed GO-QDs system based fluorometric sensing method for the detection of AA at ambient room temperature conditions.

4. Conclusion

In summary, a highly enhanced sensing platform based on QDs attached to GO was established for the detection of ascorbic acid. The GO was synthesized from graphite flakes using the modified Hummers' method. The preparation of GO-QD hybrids is simple and inexpensive. The GO and CdSe/ZnS QDs were conjugated by the EDC/Sulfo-NHS coupling reaction. FTIR and Raman spectroscopy confirmed the existence of oxygen-containing groups, and crystallinity of samples was investigated by XRD analysis. TEM analysis of GO-QDs hybrids revealed the attachment of QDs on the GO surface. The detection of ascorbic acid by GO-QDs hybrids was made possible by PL quenching resulting from electron transfer. The PL intensity of GO-QDs was sensitive to pH values and stable over a period of 4 days. The PL quenching efficiency shows a good linear relation with AA concentration with a detection limit of 568 pM and a correlation coefficient (R^2) of 0.9941. This shows that simple and sensitive detection of AA at the picomolar level is possible by using GO-QDs.

Acknowledgments: This work was supported by GRRC program (2017-A01) of Gachon University.

References

[1] Z. Gazdik, O. Zitka, J. Petrlova, V. Adam, S.B Jones, J. Zehnalek, A. Horna, V. Reznicek, M. Beklova, R. Kizek, Determination of vitamin C (ascorbic acid) using high performance liquid chromatography coupled with electrochemical detection, Sensors. 8 (2008) 7097-7112.

[2] M. Noroozifar, M. Khorasani –Motlagh, R. Akbari, M. Bemanadi Parizi, Simultaneous Voltammetric measurement of Ascorbic Acid, Epinephrine, Uric Acid and Tyrosine at a glassy carbon electrode modified with nanozeolite-multiwall Carbon Nanotube, Anal. Bioanal. Chem. Res. 1 (2014) 62-72.

[3] J.J Liu, Z.T Chen, D.S Tang, Y.B Wang, L.T. Kang, J.N. Yao, Graphene quantum dots-based fluorescent probe for turn-on sensing of ascorbic acid, Sens. Actuator B-Chem. 212 (2015) 214-219.

[4] M.B Davies, J. Austin, S.A Patridge, Vitamin C: Its Chemistry and Biochemistry, Royal Society of Chemistry Cambridge UK.

[5] T. Wu, Y. Guan, J. Ye, Determination of flavonoids and ascorbic acid in grapefruit peel and juice by capillary electrophoresis with electrochemical detection, Food Chem. 100 (2007) 1573–79.

[6] N. Anastos, N.W Barnett, B.J Hindson, C.E Lenehan, S.W Lewis, Comparison of soluble manganese (IV) and acidic potassium permanganate chemiluminescence detection using flow injection and sequential injection analysis for the determination of ascorbic acid in Vitamin C

tablets, Talanta. 64 (2004) 130–134.

[7] X. Wu, Y. Diao, C. Sun, J. Yang, Y. Wang, S. Sun, Fluorimetric determination of ascorbic acid with o-phenylenediamine, Talanta. 59 (2003) 95–99.

[8] J. Kulys, E.J D'Costa, Printed electrochemical sensor for ascorbic acid determination, Anal. Chim. Acta. 243 (1991) 173–178.

[9] S.A Kumar, P.H Lo, S.M Chen, Electrochemical selective determination of ascorbic acid at redox active polymer modified electrode derived from direct blue 71, Biosens. Bioelectron. 24 (2008) 518–523.

[10] D. Ragupathy, A.I Gopalan, K.P Lee, Electrocatalytic oxidation and determination of ascorbic acid in the presence of dopamine at multiwalled carbon nanotube–silica network–gold nanoparticles based nanohybrid modified electrode, Sens. Actuators B. 143 (2010) 696–703.

[11] D. Wen, S. Guo, S. Dong, E. Wang, Ultrathin Pd nanowire as a highly active electrode material for sensitive and selective detection of ascorbic acid, Biosens. Bioelectron. 26 (2010) 1056–61.

[12] S. Qiu, S. Gao, Q. Liu, Z. Lin, B. Qiu, G. Chen, Electrochemical impedance spectroscopy sensor for ascorbic acid based on copper (I) catalyzed click chemistry, Biosens Bioelectron. 26 (2011) 4326–4330.

[13] G. Jiang, T. Jiang, H. Zhou, J. Yao, X. Kong, Preparation of N-doped carbon quantum dots for highly sensitive detection of dopamine by an electrochemical method, RSC Advances. 5 (2015) 9064-8.

[14]. T. Jiang, G. Jiang, Q. Huang, H. Zhou, High-sensitive detection of dopamine using

graphitic carbon nitride by electrochemical method, Mater Res Bull. 74 (2016) 271-7.

[15] A.P Alivisatos, Semiconductor Clusters, Nanocrystals, and Quantum Dots, Science. 271 **(**1996) 933-937.

[16] D. Bera, L. Qian, T.K Tseng, P.H Holloway, Quantum dots and their multimodal applications: a review, Materials. 3 (2010) 2260-2345.

[17] W.C.W Chan, S. Nie, Quantum dot bioconjugates for ultrasensitive nonisotopic detection, Science. 281 **(**1998) 2016-2018.

[18] M.S Mauter, M. Elimelech, Environmental applications of carbon-based nanomaterials, Environ. Sci. Technol. 42 (2008) 5843-59.

[19] A.K Geim, K.S Nanoselov, The rise of graphene, Nat. Mater. 6 (2007) 183-191.

[20] K.S Nanoselov, A.K Geim, S.V Morozov, D. Jiang, Y. Zhang, S.V Dubonos, I.V Grigorieva, A.A Firsov, Electric field effect in atomically thin carbon films, Science. 306 (2004) 666.

[21] M. Freitag, M. Steiner, Y. Martin, V. Perebeinos, Z. Chen, J.C Tsang, P. Avouris, Energy dissipation in graphene field-effect transistors, Nano letters. 9 (2009) 1883-8.

[22] M.A. Panzer, K.E. Goodson, Thermal resistance between low-dimensional nanostructures and semi-infinite media, J. Appl. Phys. 103 (2008) 4301.

[23] M. Veerapandian, M.H. Lee, K. Krishnamoorthy, K. Yun, Synthesis, characterization and electrochemical properties of functionalized graphene oxide, Carbon. 50 (2012) 4228–38.

[24] E. Yoo, J. Kim, E. Hosono, H. Zhou, T. Kudo, I. Honma, Large reversible Li storage of graphene nanosheet families for use in rechargeable lithium ion batteries, Nano Letters. 8

(2008) 2277–82.

[25] V.K. Gupta, M.L. Yola, N. Atar, Z. Ustunda g, A.O. Solak, Electrochemical studies on graphene oxide-supported metallic and bimetallic nanoparticles for fuel cell applications, J. Mol. Liquids. 191 (2014) 172–6.

[26] Y. Yang, Y.M. Zhang, Y. Chen, D. Zhao, J.T. Chen, Y. Liu, Construction of a graphene oxide based noncovalent multiple nanosupramolecular assembly as a scaffold for drug delivery, Chem.-Eur. J. 18 (2012) 4208–15.

[27] X.X. Ma, H.Q. Tao, K. Yang, L.Z. Feng, L. Cheng, X.Z. Shi, Y. Li, L. Guo, Z. Liu, A functionalized graphene oxide-iron oxide nanocomposite for magnetically targeted drug delivery, photothermal therapy, and magnetic resonance imaging, Nano Res. 5 (2012) 199–212.

[28]. M.L Yola, V.K. Gupta, N. Atar, New molecular imprinted voltammetric sensor for determination of ochratoxin A, Mater. Sci. Eng. C. 61 (2016) 368-375.

[29]. C. Göde, M.L Yola, A. Yılmaz, N. Atar, S. Wang, A Novel Electrochemical Sensor Based on Calixarene Functionalized Reduced Graphene Oxide: Application to Simultaneous Determination of Fe (III), Cd (II) and Pb (II) Ions, J. Colloid Interface Sci. 508 (2017) 525-31.

[30]. M.L Yolaa, T. Eren, N. Atar, A novel and sensitive electrochemical DNA biosensor based on Fe@Au nanoparticles decorated graphene oxide, Elecrochim. Acta. 125 (2014) 38-47.

[31]. M.L Yola, N. Atar, Z. Ustundagˇ, A.O Solak, A novel voltammetric sensor based on p-aminothiophenol functionalized graphene oxide/gold nanoparticles for determining quercetin in the presence of ascorbic acid, J. Elecroanal. Chem. 698 (2013) 9-13.

[32] V. Georgakilas, J.N Tiwari, K.C Kemp, J.A Perman, A.B Bourlinos, K.W Klim, R. Zboril, Noncovalent functionalization of graphene and graphene oxide for energy materials, biosensing, catalytic, and biomedical applications, Chem. Rev. 116 (2016) 5464-5519.

[33]. M.L Yola, V.K Gupta, T. Eren, A.E Sen, N. Atar, A novel electro analytical nanosensor based on graphene oxide/silver nanoparticles for simultaneous determination of quercetin and morin, Elecrochim. Acta. 120 (2014) 204–211.

[34]. M.L Yola, T. Eren, N. Atar, A sensitive molecular imprinted electrochemical sensor based on goldnanoparticles decorated graphene oxide: Application to selectivedetermination of tyrosine in milk, Sens Actuators B Chem. 210 (2015) 149-157.

[35] F. Everaerts, M. Torrianni, M. Hendriks and J. Feijen, Biomechanical properties of carbodiimide crosslinked collagen: influence of the formation of ester crosslinks, J Biomed Mater Res A. 85 (2008) 547-555.

[36] F. Everaerts, M. Torrianni, M. Hendriks and J. Feijen, Quantification of carboxyl groups in carbodiimide cross linked collagen sponges, J Biomed Mater Res A. 83 (2007) 1176-1183.

[37] W.S Hummers, R.E Offeman, Preparation of graphitic oxide, J. Am. Chem. Soc. 80 (1958) 1339.

[38] S. Reghuram, A. Arivarasan, R. Kalpana, R. Jayavel, CdSe and CdSe/ZnS quantum dots for the detection of C-reactive protein, J. Exp. Nanosci. 10 (2014)787-802.

[39] Y. Si, E.T Samulski, Synthesis of water soluble graphene, Nano. Lett. 8 (2008) 1679-1682.

[40] M.S Dresselhaus, A. Jorino, M. Hofmann, G. Dresselhaus, R. Saito, Perspectives on carbon nanotubes and graphene Raman spectroscopy, Nano.Lett. 10 (2010) 751-758.

[41] A. Kundu, S. Nandi, P. Das, A.K Nandi, Fluorescent graphene oxide via polymer grafting: an efficient nanocarrier for both hydrophilic and hydrophobic drugs, ACS Appl. Mater. Interfaces. **7 (**2015) 3512.

[42] E. Jenrette, S.K Pradhan, G. Rutherford, J. Flowers, H. Duc, A.K Pradhan, Quantum-dot-conjugated graphene oxide as an optical tool for biosensor, Opt. Express. 23 (2015) 25017-25027.

[43] J. Song, L. Xu, R. Xing, Q. Li, C. Zhou, D. Liu and H. Song, Synthesis of Au/Graphene oxide composites for selective and sensitive electro chemical detection of Ascorbic acid, Scientific reports. 4 (2014) 7515.

[44] B. Lu, X. Ke, Z. Zhang, J. Hao, B. Zhang and J. Tang, Amine-assisted solvothermal approach for the insitu synthesis of metal telluride reduced graphene oxide, Carbon. 63 (2013)157-164.

[45] P. Huang, C. Xu, J. Lin, C. Wang, X. Wang, C. Zhang, X. Zhou, S. Guo, D.Cui, Folic acid conjugated graphene oxide loaded with photosensitizers for targeting photodynamic therapy, Theranostics. 1 (2011) 240-250.

[46] B.Y Chang, N.M Huang, M.N An'amt, A.R Marlinda, Y. Norazeriena, M.R Muhamad, I. Harrison, H.N Lim, C.H Chia, Facile hydrothermal preparation of titanium dioxide decorated reduced graphene oxide nanocomposite, Int J Nanomedicine. 7 (2012) 3379-3387.

[47] M. Tomasulo, I. Yildiz, F.M.R Raymo, pH-sensitive quantum dots, J Phys Chem C. 110 (2006) 3853-3855.

[48] H. Zhang, Z. Zhou, B. Yang, The influence of carboxyl groups on the photoluminescence of mercaptocarboxylic acid-stabilized CdTe nanoparticles, J Phys Chem.

B. 107 (2003) 8-13.

[49] J. Yuan, W. Guo, E. Wang, Investigation of some critical parameters of buffer conditions for the development of quantum dots-based optical sensors, Anal. Chim. Acta. 630 (2008) 174-180.

[50] P. David, T.C Werner, Jr R.M Dennin, J.K Baird, Fluorescence quenching at high quencher concentrations, J. Chem. Phys. 79 (1983) 3328.

[51] L. Zhang, G. Wang, D. Wu, C. Xiong, L. Zheng, Y. Ding, H. Lu, G. Zhang, L. Qiu, Highly selective and sensitive sensor based on an organic electrochemical transistor for the detection of ascorbic acid. Biosens. Bioelectron. 100 (2018) 235-41.

[52] D. Ji, Y. Du, H. Meng, L. Zhang, Z. Huang, Y. Hu, J. Li, F. Yu, Z. Li, A novel colorimetric strategy for sensitive and rapid sensing of ascorbic acid using cobalt oxyhydroxide nanoflakes and 3, 3′, 5, 5′-tetramethylbenzidine. Sens Actuators B Chem. 256 (2018) 512-9.

[53] W.W. Zhao, Z.Y. Ma, D.Y. Yan, J.J. Xu, H.Y. Chen, In situ enzymatic ascorbic acid production as electron donor for CdS quantum dots equipped TiO_2 nanotubes: a general and efficient approach for new photoelectrochemical immunoassay. Anal. Chem. 84 (2012) 10518-21.

Figure captions

1. Reaction scheme for the synthesis of graphene-oxide (GO) from graphite flakes (modified Hummers' method) and formation of GO-quantum dot (GO-QD) hybrids by the EDC/NHS

coupling reaction.

2. FTIR spectra of graphite (G), GO, GO-QD hybrids. Features arising from stretching and bending modes in aromatic configurations are indicated by *Ar – stre* and *Ar – bend*.

3. Raman spectra of graphite, GO, and GO-QD hybrids.

4. TEM images of (A) QDs (CdSe/ZnS), (B) graphene oxide, (C) and (D) QDs conjugated on the GO sheet at 200 and 100 nm magnification, (E) EDX spectrum of GO-QD hybrids, (F) HRTEM of GO-QD hybrids at 5 nm magnification, (**Inset** – SAED pattern GO-QDs).

5. UV-visible spectra of GO and GO-QD hybrids.

6. XRD spectra of graphite, GO, and GO-QD hybrids.

7. Maximum PL intensity of GO-QD hybrids at different pH values.

8. Maximum PL intensity of GO-QD hybrids after different continuous exposure times.

9. PL spectrum of GO-QD hybrids for various concentrations of ascorbic acid (0, 50, 60, 70, 80, 90, 100, 110, 120, and 130 nM). λ_{ex} = 450 nm. [**Inset:** (top) The linear relationship between PL intensity and ascorbic acid concentrations, (bottom) photographic images of the PL quenching by addition of AA].

10. Response of PL emission spectra for the various biomolecules (A) and ions (B) as potential interferences.

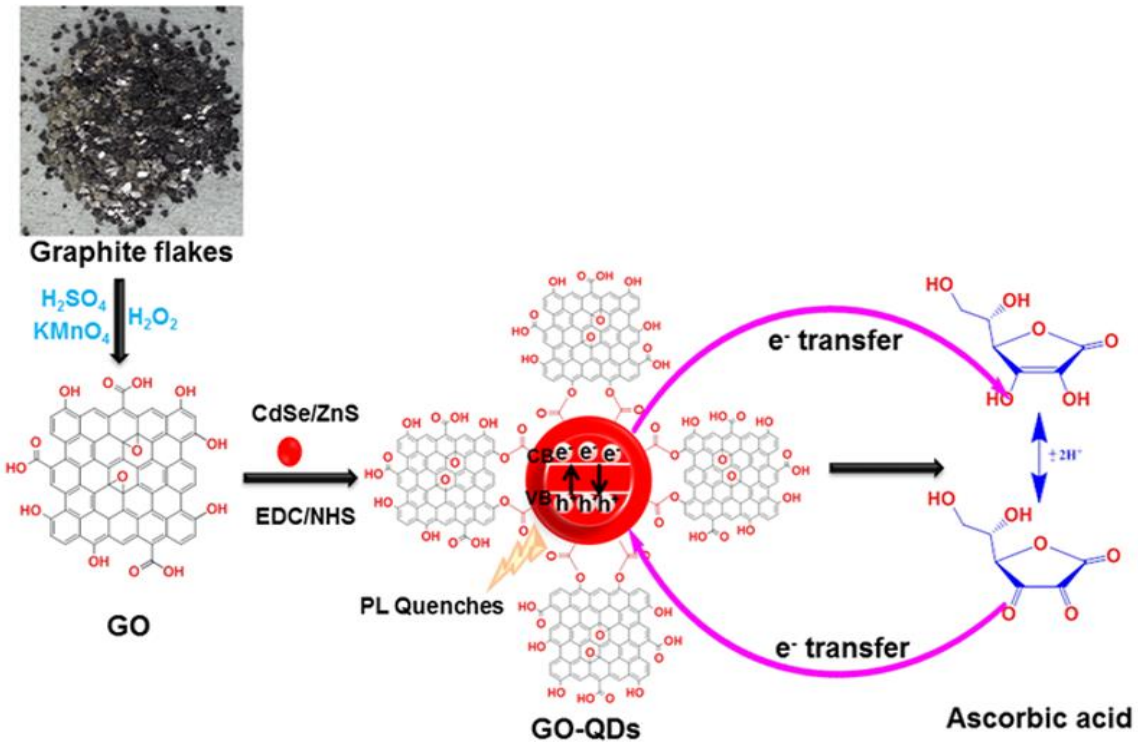

Fig. 1

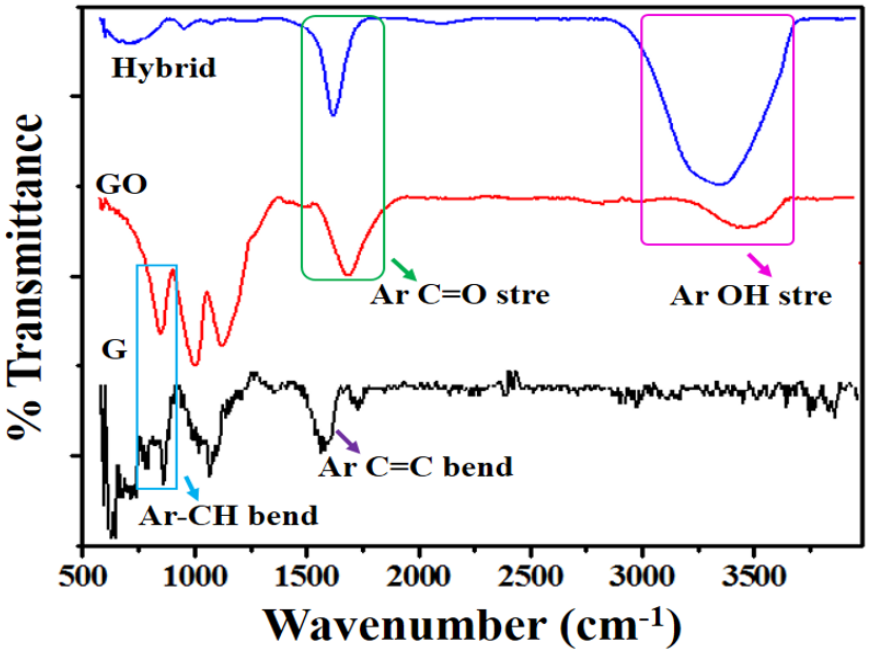

Fig. 2.

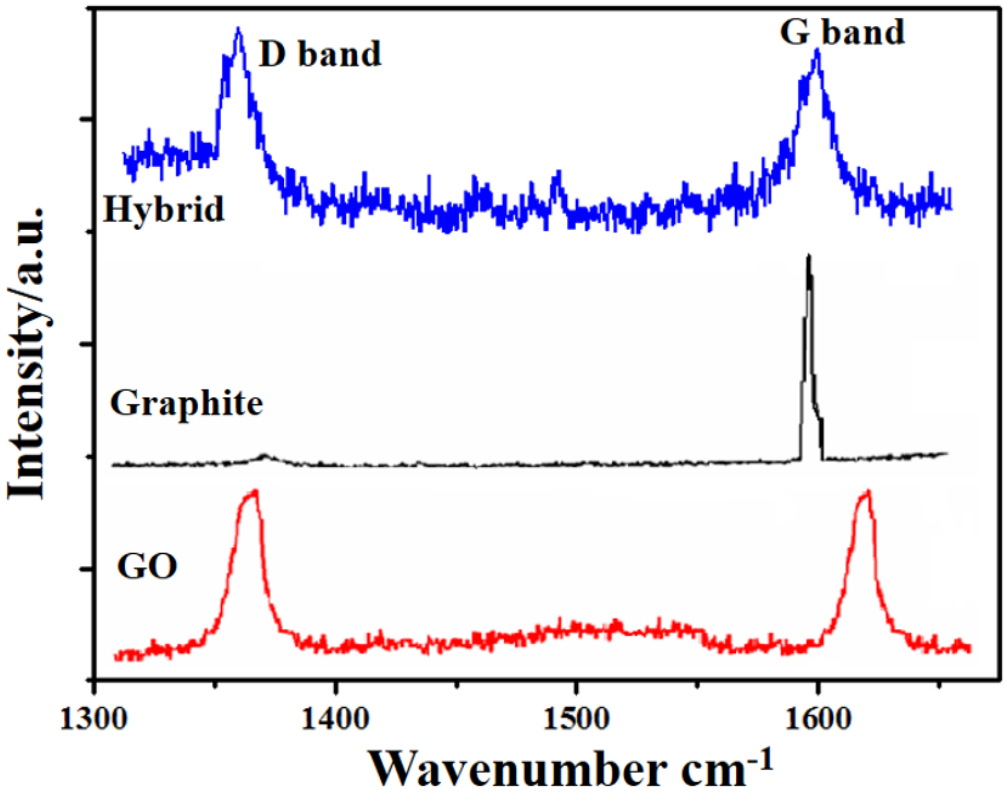

Fig. 3

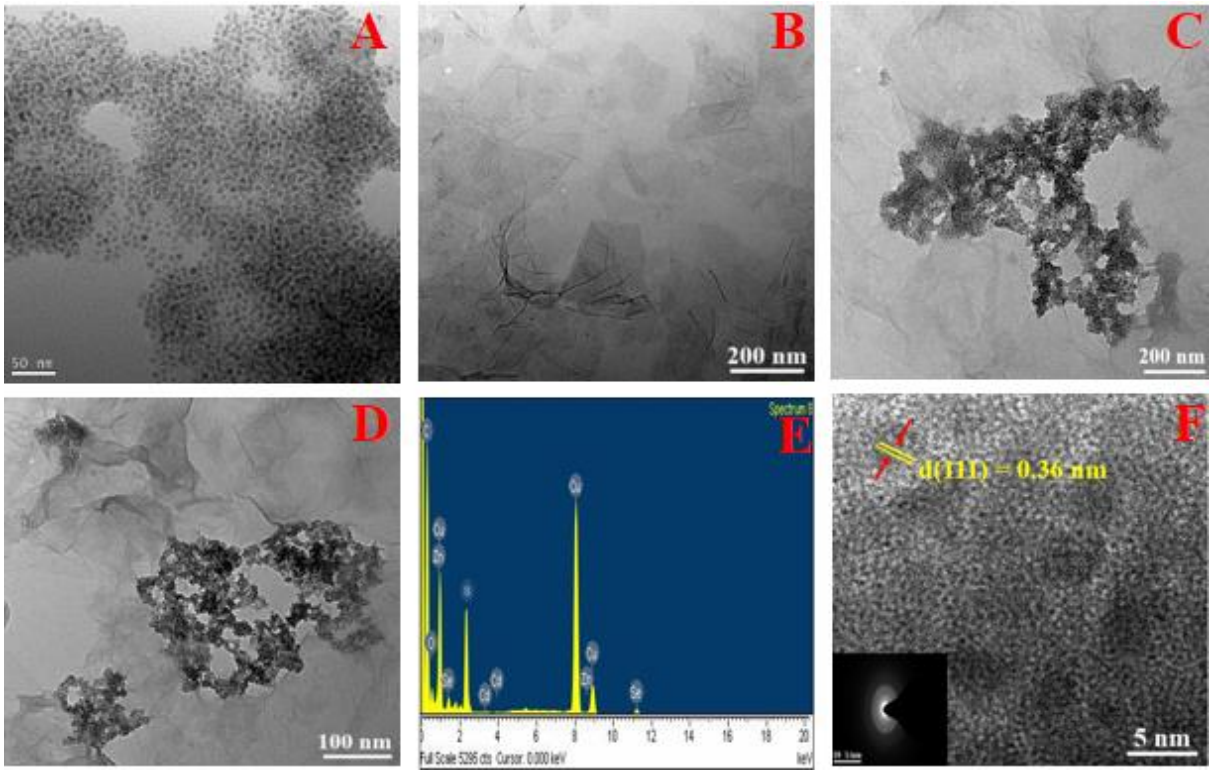

Fig. 4

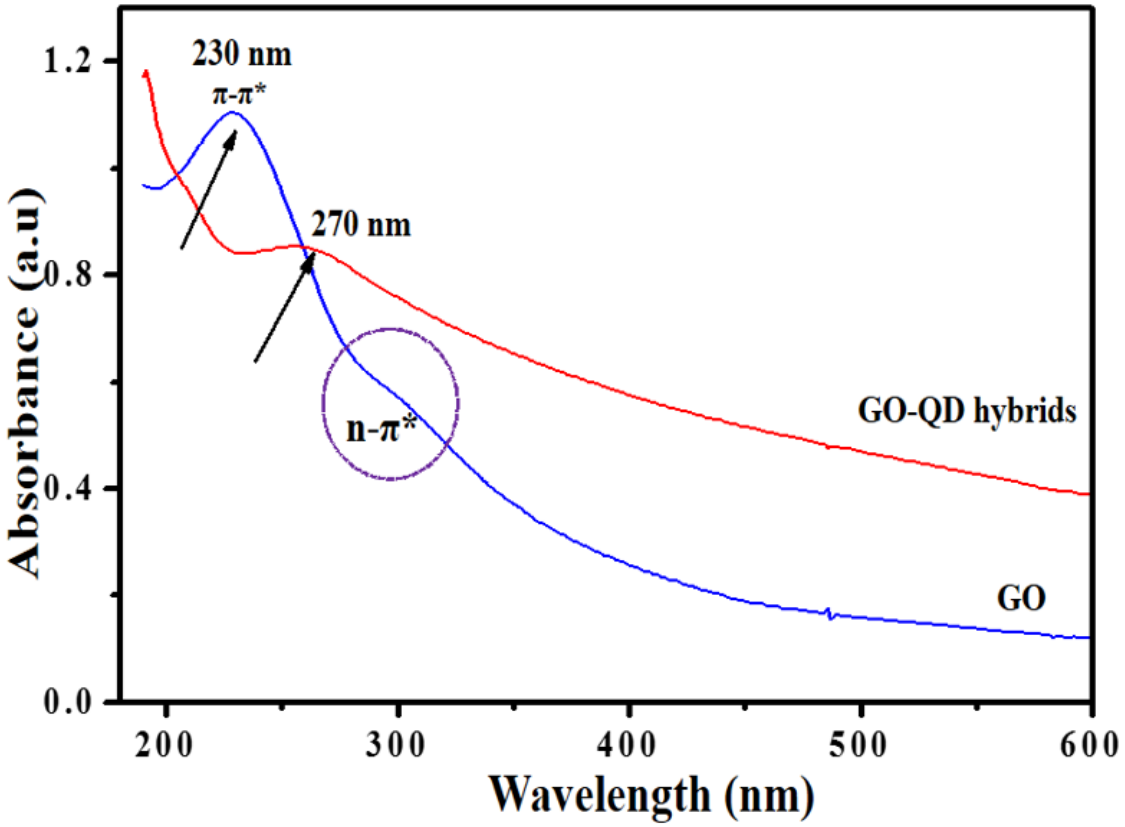

Fig. 5

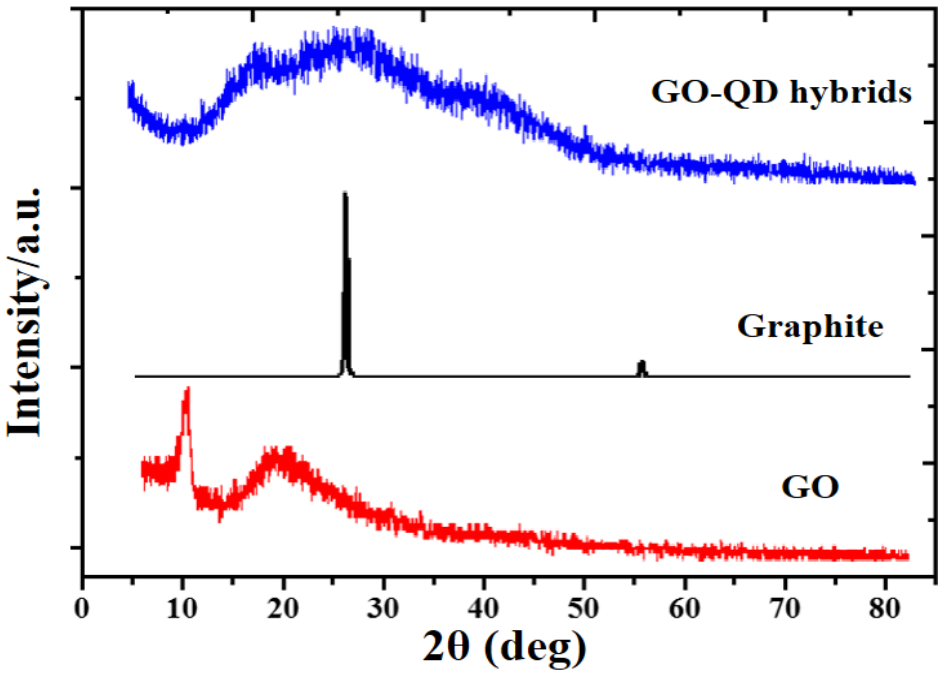

Fig. 6

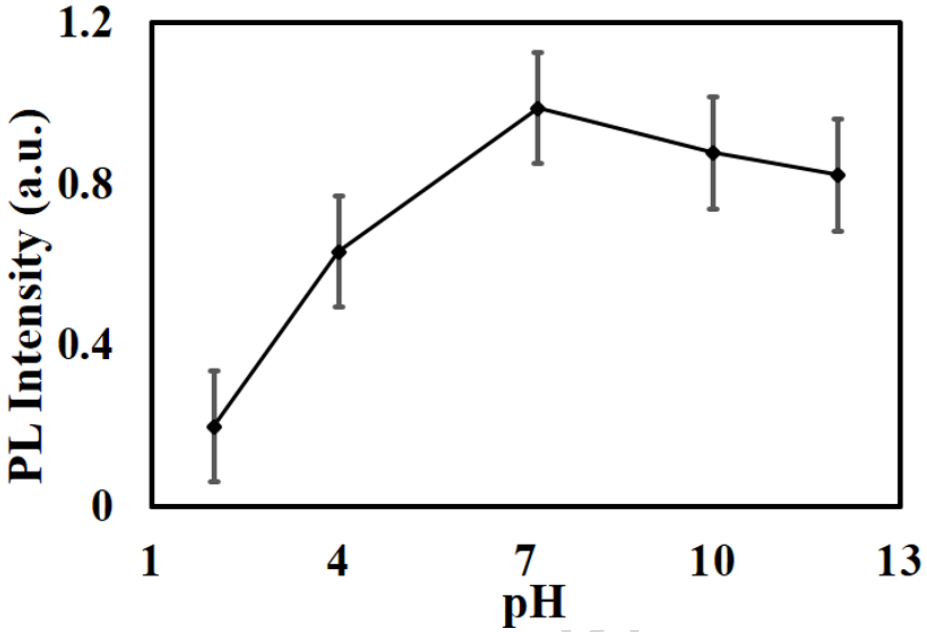

Fig. 7

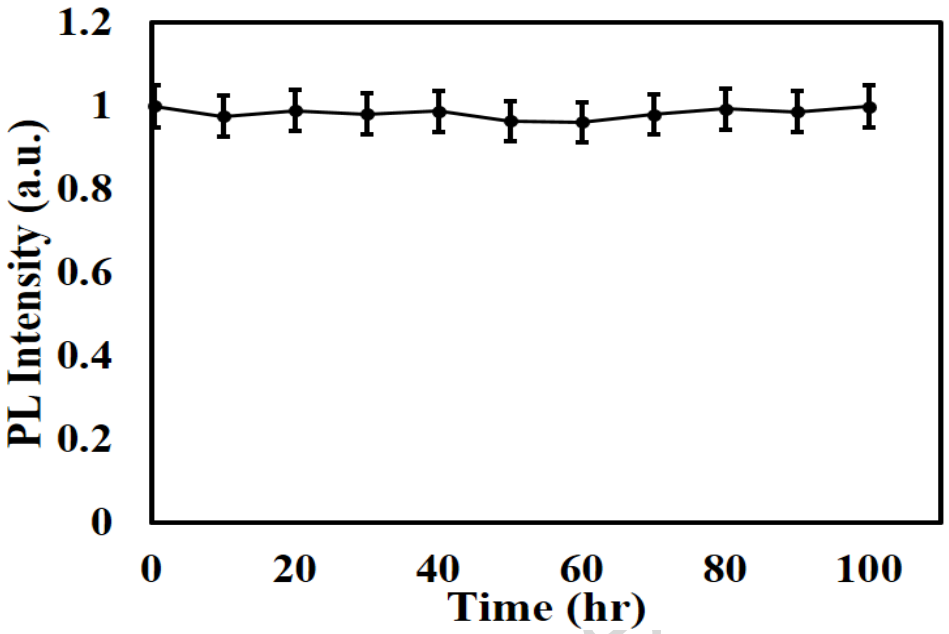

Fig. 8

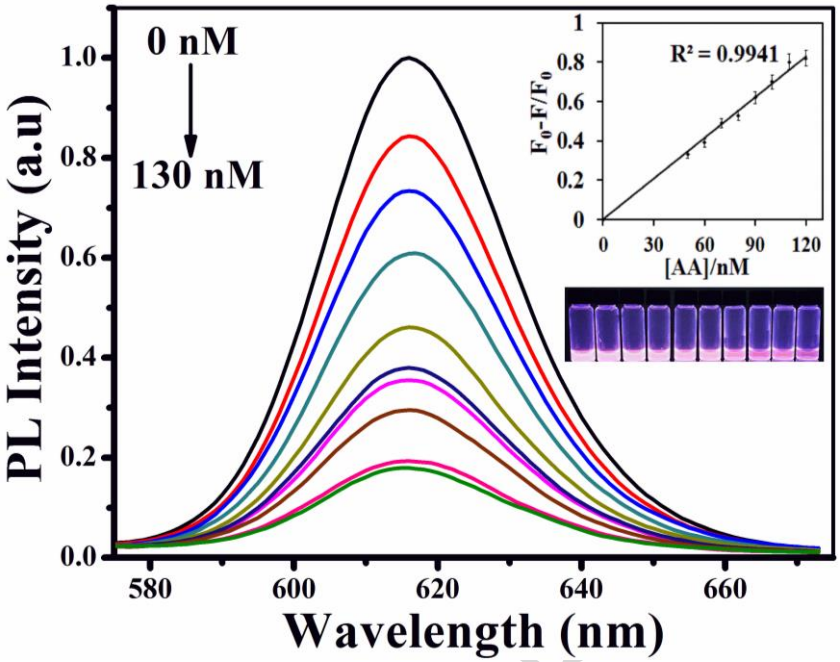

Fig. 9

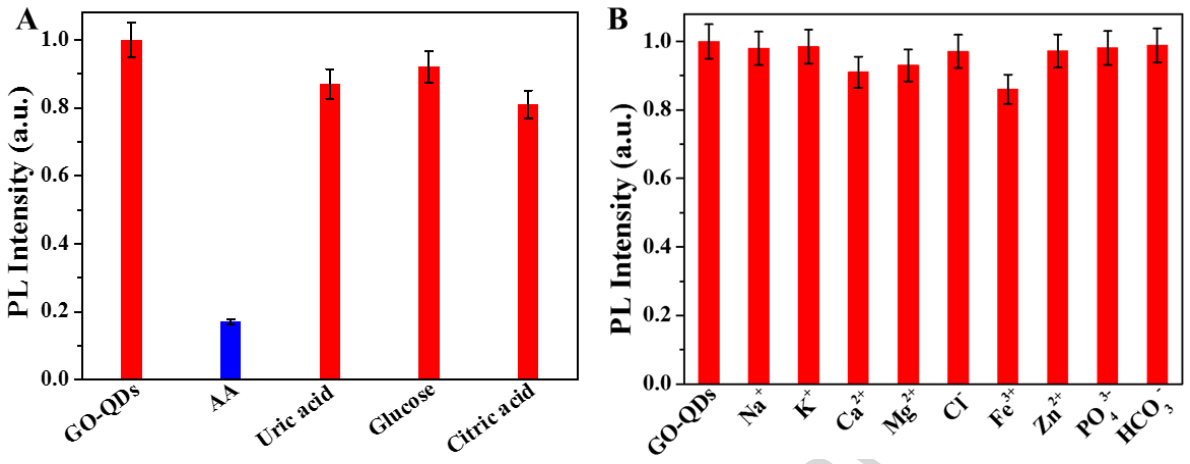

Fig. 10

Highlights

- Sensing platform based on quantum dots attached to graphene oxide (GO) was established
- The preparation of GO-QD hybrids is simple and inexpensive.
- As-prepared GO-QD hybrids are successful in detecting ascorbic acid
- Simple and sensitive detection of ascorbic acid at picomolar level